

# Neutral hydrogen in galactic fountains

C. M. Booth<sup>1\*</sup>, Tom Theuns<sup>1,2</sup>

<sup>1</sup>*Institute for Computational Cosmology, University of Durham, South Road, Durham DH1 3LE*

<sup>2</sup>*University of Antwerp, Campus Groenenborger, Groenenborgerlaan 171, B-2020 Antwerpen, Belgium*

2 November 2018

## ABSTRACT

Simulations of an isolated Milky Way-like galaxy, in which supernovae power a galactic fountain, reproduce the observed velocity and 21 cm brightness statistics of galactic neutral hydrogen (HI). The simulated galaxy consists of a thin HI disk, similar in extent and brightness to that observed in the Milky Way, and extra-planar neutral gas at a range of velocities due to the galactic fountain. Mock observations of the neutral gas resemble the HI flux measurements from the Leiden-Argentine-Bonn (LAB) HI survey, including a high-velocity tail which matches well with observations of high-velocity clouds. The simulated high-velocity clouds are typically found close to the galactic disk, with a typical line-of-sight distance of 13 kpc from observers on the solar circle. The fountain efficiently cycles matter from the centre of the galaxy to its outskirts at a rate of around  $0.5M_{\odot}\text{yr}^{-1}$ .

**Key words:** galaxies: ISM — ISM: clouds — methods: N-body simulations

## 1 INTRODUCTION

Radio observations of the 21 cm hydrogen emission line reveal that the Milky Way (MW) contains a thin HI disk surrounded by a population of ‘clouds’ with velocities incompatible with models of galactic rotation yet apparently not part of the Hubble flow either (Muller et al (1963)). The nature of these ‘high-velocity clouds’ (HVCs) remains somewhat unclear mostly because it is difficult to determine their distances and hence infer physical properties.

Observations of stars with known distances along the line of sight to a HVC can be used to constrain the distance to the cloud, by testing whether or not it is detected in absorption in the stellar spectrum (see e.g. Schwarz et al (1995)). Unfortunately such constraints are available for only a relatively small number of HVCs (Wakker (2001)). Putman et al. (2003) use constraints from H $\alpha$  emission, and find that most HVCs are within  $\sim 40$  kpc, except for those associated with the Magellanic stream. Brüns et al. (2001) claim that some fraction of HVCs display a head-tail morphology, may be a result of interaction with a diffuse ambient galactic wind (Quilis & Moore (2001)). Searches for stars associated with HVCs have so far resulted in non-detections (e.g. Hopp et al. (2007)). Metallicities have been measured for a small number of HVCs and vary over a wide range (e.g. Gibson et al. (2001)), suggesting that HVCs are not a homogeneous set. Finally one can observe other galaxies to infer the nature of HVCs from their projected dis-

tances. The Andromeda galaxy (M31) has a population of HVCs close ( $\leq 50$  kpc) to its disk (Westmeier et al. (2007)). Other nearby spiral galaxies also contain extra-planar neutral gas (see e.g. Barbieri et al. (2005)). Pisano et al. (2007) have searched for HVC analogues in six loose groups of galaxies, similar to the Local Group. Their failure to detect compact HVCs implies that any HI clouds are near to the galaxies in this group: they are not roaming freely throughout the group itself. These observations do not unambiguously determine the nature of HVCs, and several theoretical models for them have been proposed. Oort (1970) discusses a model where the HVCs are close to the MW disk, and result from a ‘galactic fountain’ (Shapiro & Field (1976)). Gas from the galactic disk rises buoyantly after being heated by supernovae (SNe), becomes thermally unstable and cools radiatively into neutral clouds. Once the clouds are dense they fall back ballistically onto the disk, and are seen as the HVCs. Whether SNe explosions can start a galactic fountain has been investigated both theoretically (Kahn (1998)) and through numerical simulations (de Avillez (1998); de Avillez & Berry (2001)).

Blitz et al. (1999; see also Braun & Burton (1999)) suggest (some) HVCs are neutral gas associated with the numerous dark matter substructures seen in simulations of haloes of galaxies and groups of galaxies. Such HVCs are at large distances ( $\gtrsim 40$  kpc) from the galactic centre, and distributed throughout the local group. Connors et al (2006) report the detection of HI clouds in fully cosmological  $\Lambda$ CDM simulations of galaxy formation, and their HVCs are reminiscent of Blitz’s clouds. Maller & Bullock

\* E-mail: c.m.booth@durham.ac.uk (CMB)

(2004) discuss how a population of clouds at distances of  $\sim 150$  kpc may result from the halo gas becoming thermally unstable. Given the rich variety HVC properties it seems likely that more than one of the above models, with an additional component resulting from tidal interactions (e.g. Ferguson et al. (2006)) is required to explain the full cloud distribution. In this letter we perform numerical simulations of star formation in an isolated Milky Way-like galaxy, in which SNe power a galactic fountain. We analyse the simulation in terms of mock H I observations and demonstrate they reproduce many of the observed features of the H I disk and its HVCs.

This letter is structured as follows. In section 2 we provide details of the numerical scheme used in our investigation and in section 3 we present a comparison between our simulations and the distribution of galactic H I.

## 2 NUMERICAL METHOD

### 2.1 Star Formation and Feedback model

The star formation and feedback prescriptions used in the simulations is described in detail in Booth et al (2007) (hereafter BTO07), here we briefly review its main features. The scheme treats the interstellar medium (ISM) in terms of three distinct but interacting components: cold ( $T \lesssim 10^2$  K) molecular clouds surrounded by a warm ( $T \sim 10^4$  K) ambient phase in the disk, interspersed by a hot ( $T \sim 10^6$  K) tenuous phase that extends into the halo, and is powered by SNe. Gas is cycled through these phases by a number of processes.

Conversion of gas to stars is regulated by the rate at which molecular clouds form and get destroyed. Clouds form from thermally unstable ambient gas and get destroyed directly by feedback from massive stars, and indirectly through thermal conduction. Gas cooling is due to Compton and line cooling, using interpolation tables generated using CLOUDY<sup>1</sup> (Ferland et al. (1998)). Feedback in the ambient gas phase cycles gas into a hot galactic fountain or wind. We model the ambient and hot gas phases hydrodynamically using smoothed particle hydrodynamics (SPH, Gingold & Monaghan (1977); Lucy (1977)) as implemented in the GADGET2 simulation code (Springel (2005)). Motivated by the fact that we cannot resolve the Jeans mass of the molecular gas, the clouds are modelled using ‘sticky particles’ that move ballistically through the ambient gas, but may coagulate when colliding. When such a cloud has built-up enough mass through accretion and coagulation to form a Giant Molecular Cloud (GMC), it collapses into stars, which then destroy the GMC through stellar winds and SNe explosions.

BTO07 show that this model produces a multiphase medium with cold clouds, a warm disk, hot SN bubbles and a hot, tenuous halo, similar to that observed in spiral galaxies. The star formation rate, surface H I density, molecular fraction, and molecular cloud mass-spectrum of simulated galaxies match closely those observed in the MW.

<sup>1</sup> We thank our colleagues J Schaye, C Dalla Vecchia and R Wiersma for allowing us to use these routines.

### 2.2 Model Galaxy

The initial conditions for our MW-like galaxy are generated using a publicly available programme, GALACTICS (Kuijken & Dubinski (1995)), which generates a near equilibrium galaxy consisting of an approximately exponential disk, a bulge and a (dark matter) halo, using collisionless particles. The bulge, disk and halo have masses in the ratio 0.31:1.00:28.27 (giving a baryon fraction of  $\sim 0.3$  times the universal value). The total mass of the system is  $2.21 \times 10^{12} M_{\odot}$  and the circular velocity at the solar radius,  $r = 8.5$  kpc, is  $\sim 220 \text{ km s}^{-1}$ .

We convert 10% of the disk particles into SPH particles with temperature  $10^4$  K, the remaining 90% of the disk represents a stellar disk with population ages set by assuming that the galaxy had a constant star formation rate of  $1 M_{\odot} \text{ yr}^{-1}$ . The bulge is changed in its entirety into an old stellar population. Finally 1% of the material in the halo is changed into SPH particles with a temperature of  $10^6$  K. The galaxy is now no longer in equilibrium and starts converting atomic gas into molecular clouds, which in turn form stars, yet soon settles into a near-equilibrium state where feedback regulates the star formation rate at approximately  $1 M_{\odot} / \text{yr}$ . It was shown in BTO07 that the resulting galaxy resembles the MW in terms of its gas fraction, molecular fraction, gas distribution and Schmidt-Kennicutt star formation law. Our highest resolution simulation initially contains  $\sim 3 \times 10^6$  particles in the disk (particle mass  $\approx 1.5 \times 10^5 M_{\odot}$ ), but it has been demonstrated in BTO07 that the properties of this galaxy are not strongly dependent on resolution.

### 2.3 Mock H I observations

We assume that the H I fraction of the ambient gas is set by the balance between photo-ionisation, collisional ionisation, and recombinations, which we compute using CLOUDY (Ferland et al. (1998)), imposing the UV background at redshift  $z = 0$  given by Haardt & Madau (2001). This H I gas can be detected by its hyperfine emission line (Van de Hulst (1945)). A hydrogen atom in its ground state has higher energy when the spins of proton and electron,  $J_p$  and  $J_e$ , are parallel than when they are anti-parallel. Spontaneous transitions to the lower energy state occur at a rate governed by the Einstein coefficient,  $A_{10} = 2.85 \times 10^{-15} \text{ s}^{-1}$ , and result in the emission of a ‘21 cm photon’ of wavelength  $\lambda = 21.11 \text{ cm} = c/\nu$ . For the densities,  $n_{\text{H}}$ , and temperatures,  $T$ , relevant to the ISM, the typical time  $\tau$  between collisions,  $\tau \sim 100 \times (n_{\text{H}}/\text{cm}^{-3})^{-1} (T/10^4 \text{ K})^{-1/2} \text{ yr}$ , is much shorter than the spontaneous 21cm transition rate,  $\tau_{1/2} = A_{10}^{-1} \text{ s} \sim 10^7 \text{ yr}$ , and so collisions keep the levels of the low and high states,  $n_0$  and  $n_1$ , in the ratio  $n_1 = 3n_0$ . The mean emission rate of 21 cm photons per neutral hydrogen is then given by  $A_{10} n_1 = (3/4) A_{10}$ . The 21 cm flux of a cloud with neutral hydrogen mass  $M_{\text{HI}}$  at distance  $D$  is

$$F = \frac{(3/4) A_{10} (M_{\text{HI}}/m_{\text{H}}) h\nu}{4\pi D^2} \approx 2 \times 10^{-19} \frac{M_{\text{HI}}}{M_{\odot}} \left(\frac{1 \text{ kpc}}{D}\right)^2 \text{ erg cm}^{-2} \text{ s}^{-1}, \quad (1)$$

(see e.g. Spitzer (1978)). In radio astronomy, this is quoted in terms of the line flux,  $\int S(\nu) d\nu$ , with  $S(\nu)$  expressed in Jy and the line-width in  $\text{km s}^{-1}$ ,  $F = \int S(\nu) d\nu =$

$\int S(\nu) (\nu/c) d\nu$ , hence (Wakker & van Woerden (1991))

$$\int \left[ \frac{S(\nu)}{\text{Jy}} \right] \left[ \frac{d\nu}{\text{kms}^{-1}} \right] = \frac{1}{\text{Jy}} \frac{1}{\text{kms}^{-1}} \frac{c}{\nu} F \quad (2)$$

$$= \frac{1}{0.235} \frac{M_{\text{HI}}}{M_{\odot}} \left( \frac{\text{kpc}}{D} \right)^2. \quad (3)$$

The 21cm ‘brightness temperature’,  $T_B$ , of an object is defined as the temperature at which a black-body emits the same flux. The conversion from flux to brightness temperature is then given by  $T_B/S = R$ , where the telescope-dependent conversion factor we use is  $R = 0.158\text{K Jy}^{-1}$  in order to match the observational survey we are comparing our results against (Hulsbosch & Wakker (1988)). To compute the simulated H I flux we place an observer in the simulated galaxy and evaluate the net flux received by an ideal radio telescope with a beam size  $\theta$ . For a single SPH particle at position  $\mathbf{r}_i$ , the fraction  $dm/m$  of mass that falls within the beam at distance between  $r$  and  $r + dr$  is

$$dm/m = \left( 2\pi r^2 (\cos(\theta) - 1) dr \right) W(|\mathbf{r}_i - \mathbf{r}|, h), \quad (4)$$

where  $h$  is the smoothing length of the particle, and  $W$  the SPH kernel. The total flux received from this particle is computed from Eq. (1), and is represented by a Gaussian emission line centred at velocity  $\mathbf{v} \cdot \mathbf{r}/r$  with width  $\sigma_v = (k_B T/m_h)^{1/2}$ . The total spectrum is obtained integrating over  $dr$  and summing over all particles.

Simulations have been performed at two different mass resolutions to ensure that resolution effects do not affect our results. Observations have been repeated for a number of observers along the solar circle, and at times spanning a period of 1Gyr. We use these observers to compute error bars on the mock observations. The distribution of H I at galactic latitudes,  $b$ , greater than  $20^\circ$  does not depend strongly on the time at which observations are made, showing that the galaxy our results do not represent a transient feature. Within the galactic disk ( $b < 20^\circ$ ) the mean brightness temperature of the gas decreases slowly over time as the gas disk is converted into stars.

### 3 RESULTS AND DISCUSSION

The all-sky 21 cm brightness distribution of the simulated galaxy looks remarkably similar to the observed H I in the Milky Way, as measured by the Leiden-Argentine-Bonn (LAB, Kalberla et al (2005)) H I survey (Fig. 1). The LAB survey has angular resolution of  $0.5^\circ \times 0.5^\circ$  but unfortunately our numerical simulation does not have enough particles to resolve structures on such small scales. We calculate the mean angular extent of the particles that contribute to the flux in a given direction on the sky in the simulated galaxy, and then smooth the LAB survey with a Gaussian kernel of the same width. At low galactic latitudes this smoothing angle is typically less than  $1^\circ$ . However, at high latitudes the mean smoothing length is much larger, and at  $|b| > 60^\circ$  can reach up to  $20^\circ$  due to the relatively small number of SPH particles at these latitudes.

Both observed and simulated brightness maps display a bright and thin H I disk in the plane of the MW, embedded in a thicker cooler envelope ( $T_B \sim 10^3$  K), with an even cooler component ( $T_B \sim 100$  K) at high velocities,  $|v_{\text{lsr}}| > 100$  km  $\text{s}^{-1}$ , with respect to the local standard of rest (LSR). The

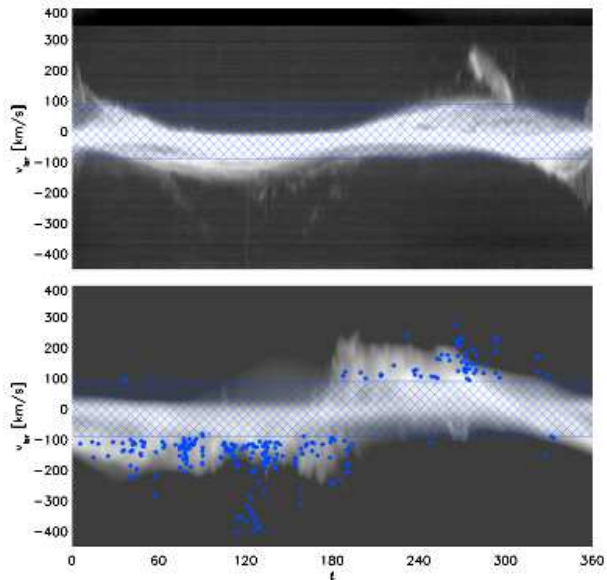


**Figure 2.** Velocities with respect to the local standard of rest of H I gas in the LAB survey (top panel) and the simulated galaxy (bottom panel) as function of galactic longitude,  $l$ . Intensity on this plot is the 21cm brightness of the H I, integrated over galactic latitude. The simulated galaxy has H I gas out to velocities of  $|v_{\text{lsr}}| \sim 200$  km  $\text{s}^{-1}$  in a characteristic pattern also seen in the LAB. The blue points (bottom panel) are HVCs from the catalogue of Lockman et al (2002). The simulation does not resolve small clouds, but the velocity distribution of the simulated H I traces the same regions in  $(l, v_{\text{lsr}})$  space as the observed clouds.

brightness temperature  $T_B$ , and its fall-off with latitude, is very similar in the observed and simulated maps. The minimum H I brightness temperature in the simulated map is 95K, in good agreement with H I observations of the MW, where it is found that every line-of-sight contains easily observable H I. The simulated high velocity gas ( $|v_{\text{lsr}}| > 100$  km  $\text{s}^{-1}$ ) forms a nearly uniform background. Due to the relatively small number of particles that are flagged as high velocity at any one time the spatial resolution is poor, especially at high latitudes, and these simulations do not resolve the fine structure seen in the LAB. When the LAB data are smoothed to the same resolution as the simulation the resulting distribution matches closely, with a mean brightness temperature of  $T_B \sim 23.22$  K, as compared to 20.33 K in the simulations.

The velocity distribution of the simulated H I also matches well with the LAB data (Fig 2). Although we cannot resolve individual HVCs, the simulated H I velocities are in good agreement with the properties of the HVC catalogue of Lockman et al (2002). Lockman et al (2002) identified some of the detections in this survey with external galaxies, we have removed these from the plot. Additionally, clouds that were identified as being part of the Magellanic stream, which dominate the extreme negative velocity flow (Mathewson, Cleary, & Murray (1974)), were removed.

The line flux,  $\int S(\nu) d\nu$ , for high velocity gas,  $|v_{\text{lsr}}| > 100$  km  $\text{s}^{-1}$ , is shown in Fig. 3. Solid black lines represent the results of Wakker (1991) with the emission due to the Magellanic stream and outer arm of the MW removed, as we do not expect an isolated galaxy to match these fea-

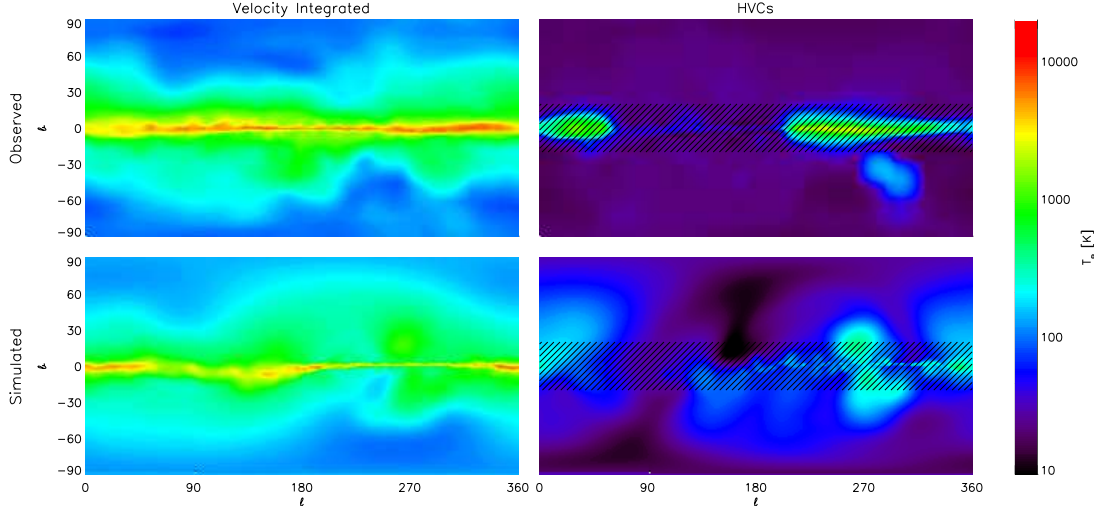


**Figure 1.** All-sky maps of 21 cm brightness temperatures in the LAB survey (top panels) and in simulations (lower panels), integrated over all velocities (left panels) or integrated over high velocities ( $|v_{\text{lsr}}| > 100 \text{ km s}^{-1}$ ) only (right panels). The observational data has been convolved with a spatially adaptive Gaussian, to make the angular resolution of both the simulated and observed data the same. Both observed and simulated galaxy consist of a thin ( $b < 5^\circ$ ) H I disk with brightness temperature  $T_B > 5000 \text{ K}$ , embedded in a thicker ( $b \sim 45^\circ$ ) disk with  $T_B \sim 1000 \text{ K}$ , with  $T_B \sim 100 \text{ K}$  at higher latitudes. The high velocity gas has  $T_B \lesssim 100 \text{ K}$  in both observed and simulated galaxy. The simulation does not reproduce the smaller-scale structure seen in the LAB due to lack of numerical resolution.

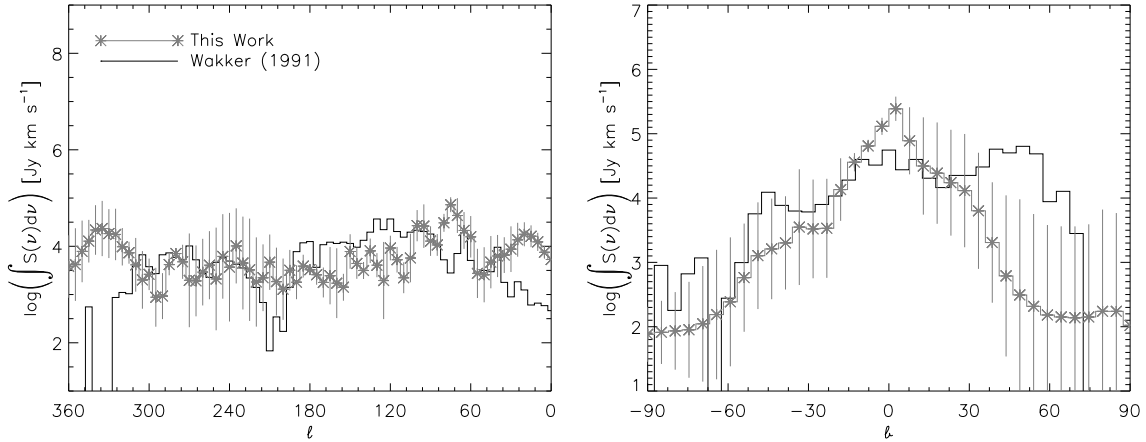


**Figure 3.** Line flux of 21 cm emission in galactic longitude  $l$  (left panel) and latitude  $b$  (right panel) for high velocity gas. The solid black lines are from the survey for HVCs by Wakker (1991). The observational data has the populations of clouds belonging to the Magellanic stream and outer arm removed, as an isolated MW galaxy can not reproduce these. The grey histogram is obtained from the simulations, with error bars a measure of the scatter between simulated observers at the solar circle. The simulated galaxy looks very similar to the observed one in  $l$ , but the distribution in  $b$  is slightly more extended in the real MW, although the simulated scatter is large.

tures. Errors on the mock data are calculated by repeating the measurements for observers at different points along the solar circle. The mock and real data look remarkably similar. The distribution of neutral gas perpendicular to the galactic plane is approximately exponential with a scale height of 5 kpc, in agreement with the predictions of Bregman (1980) for a galactic fountain. Although as noted in Fig 3 the distribution of 21cm emission in galactic latitude is slightly more concentrated in the simulated data than the observed data, when averaged over the whole sky the mean values of the smoothed maps agree to within 10% and are 485K for the observed data, and 446K for the simulated data.

It is difficult to measure the distances to HVCs in the real universe. However, in our simulations this information

is preserved and can be measured easily (Fig 4). 50% of the flux is emitted within a distance of 13 kpc from our observer. This figure is in line with that observed other galaxies (Barbieri et al. (2005); Pisano et al. (2007)), notably in M 31 by Westmeier et al (2005), who found that HVCs were generally at a projected distance of less than 15 kpc.

Gas in the fountain rains back on the disk at a radius ( $r_{\text{returned}}$ ) which is generally larger than the radius ( $r_{\text{ejected}}$ ) from where it was launched (Fig 5). An SPH particle is classified as being part of the fountain if it is ejected to a vertical distance of more than 2 kpc from the galactic plane and at a later time falls back within 1 kpc of the galactic disk. The galactic fountain has an overall effect of moving gas from the inner part of the galactic disk to its outskirts: most fountain

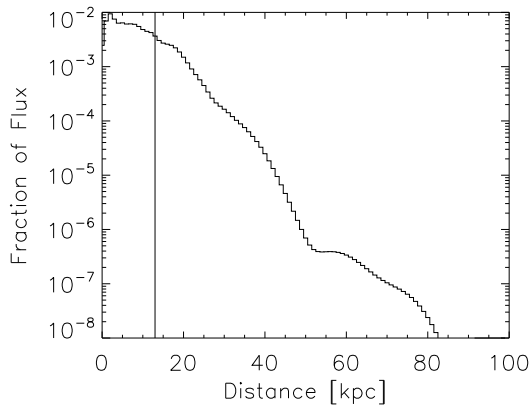


**Figure 4.** Flux weighted mean distance to H I emitting high velocity ( $|v_{\text{lsr}}| > 100 \text{ km s}^{-1}$ ) gas in the simulated galaxy. Fifty per cent of the emission occurs within  $\sim 13 \text{ kpc}$  (vertical line).

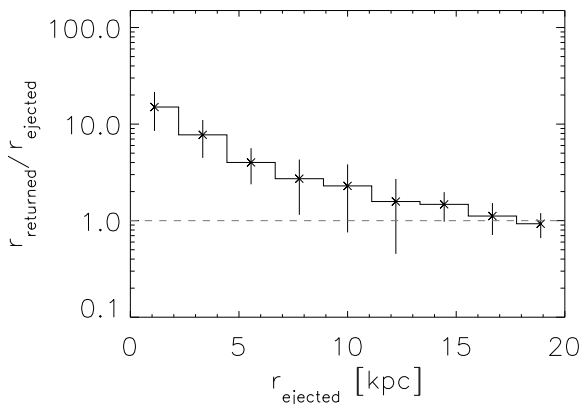


**Figure 5.** Histogram showing the relation between the galactic radius at which gas is ejected from the galaxy ( $r_{\text{ejected}}$ ), and the radius at which it next passes through the galactic disk ( $r_{\text{returned}}$ ). Overall the galactic fountain acts to move gas from the centre of the galactic disk to its outskirts.

particles with  $r_{\text{ejected}} < 8 \text{ kpc}$  have  $r_{\text{returned}}/r_{\text{ejected}} \gtrsim 4$  hence rain back outside the solar circle. Corbelli & Salpeter (1988) note that the effect of this ‘outer galactic fountain’ depends upon the physical properties of the gas that returns to the disk at large radii and could either evaporate the H I disk, or cause it to grow. The rate at which gas returns to the outer disk in the simulations,  $\dot{M} \sim 0.5 M_{\odot} \text{ yr}^{-1}$ , is in agreement with observational estimates and could be enough to drive the observed turbulence (Santillán et al. (2007)). We find that a peak mass flux of at least  $0.5 M_{\odot} \text{ yr}^{-1}$  through the disk out to a radius of 15 kpc, suggesting that a galactic fountain of this form is capable of driving ISM turbulence all the way to the outskirts of the galactic disk. In our simulations,  $\dot{M}$  decreases gradually as the quiescent star formation rate gradually decreases due to the depletion of the local gas supply. However, we note that in a fully cosmological setting bursts of star formation due to galaxy mergers coupled with infall of gas from the surrounding intergalactic medium could continue to drive this process over the lifetime of the galaxy.

We conclude that our multi-phase star formation implementation naturally produces a galactic fountain in a Milky Way-like model galaxy. The neutral hydrogen in the foun-

tain has a spatial and velocity distribution in good agreement with a variety of observations for the MW and other spiral galaxies.

## ACKNOWLEDGEMENTS

CB thanks PPARC for the award of a research studentship.

## REFERENCES

- Barbieri, C. V. et al. 2005, AAP, 439, 947  
 Brüns, C., Kerp, J., & Pagels, A. 2001, AAP, 370, L26  
 Connors T. W. et al. 2006, ApJ, 646, 53  
 Corbelli, E., Salpeter E. E., 1988, ApJ, 326, 551  
 Blitz L., et al., 1999, ApJ, 514, 818  
 Booth C. M., Theuns T., Okamoto T., 2007, MNRAS, 376, 1588  
 Braun R., Burton W. B., 1999, AAP, 341, 437  
 Bregman J. N., 1980, ApJ, 236, 577  
 de Avillez M. A., 1998, Ap&SS, 261, 201  
 de Avillez M. A., Berry D. L., 2001, MNRAS, 328, 708  
 Ferguson, A. M. N. et al. 2006, Planetary Nebulae Beyond the Milky Way, Springer, 286  
 Ferland, G. J. et al. 1998, PASP, 110, 761  
 Gibson B. K et al. 2001, AJ, 122, 3280  
 Gingold, R. A., Monaghan, J. J., 1977, MNRAS, 181, 375  
 Haardt, F., & Madau, P., 2001, Clusters of Galaxies and the High Redshift Universe Observed in X-rays  
 Hopp, U., Schulte-Ladbeck, R. E., & Kerp, J. 2007, MNRAS, 374, 1164  
 Hulsbosch A. N. M., Wakker B. P., 1988, A&AS, 75, 191  
 Kahn F. D., 1998, The Galactic Fountain, IAU Colloq. 166: The Local Bubble and Beyond, Berlin Springer Verlag  
 Kalberla P. M. W. et al. 2005, AAP, 440, 775  
 Kuijken K., Dubinski J., 1995, MNRAS, 277, 1341  
 Lockman F. J., Murphy E. M., Petty-Powell S., Urlick V. J., 2002, ApJS, 140, 331  
 Lucy, L. B, 1977, AJ, 82, 1013  
 Maller A. H., Bullock J. S., 2004, MNRAS, 355, 694  
 Muller, C.A., Oort, J.H., Raimond, E., 1963, CR Paris 257  
 Mathewson D. S., Cleary M. N., Murray J. D., 1974, ApJ, 190, 291  
 Oort J. H., 1970, AAP, 7, 381  
 Pisano, D. J., et al., 2007, ApJ, 662, 959  
 Putman, M. E. et al 2003, ApJ, 597, 948  
 Quilis V., Moore B., 2001, ApJ, 555, L95  
 Santillán, A., Sánchez-Salcedo, F. J., & Franco, J. 2007, ApJL, 662, L19  
 Schwarz U. J., Wakker B. P., van Woerden H., 1995, AAP, 302, 364  
 Shapiro P. R., Field G. B., 1976, ApJ, 205, 762  
 Spitzer, L. 1978, New York, Wiley-Interscience, 1978  
 Springel V., Yoshida N., White S. D. M., 2001, NewA, 6, 79  
 Springel V., 2005, MNRAS, 364, 1105  
 Van de Hulst, H. C., 1945, Nederl. Tij. Natuurkunde, 11, 201  
 Wakker B., 1991, AAP, 250, 499  
 Wakker B., 2001, ApJs, 136, 463  
 Wakker B., van Woerden H., 1991, AAP, 250, 509  
 Westmeier T., Braun R., Thilker D., 2005, AAP, 436, 101  
 Westmeier, T. et al. 2007, New Astronomy Review, 51, 108